J|A|C|S
COMMUNICATIONS

Published on Web 08/24/2006

Unusual Non-Bulk Properties in Nanoscale Materials: Thermal Metal−Metal Bond Contraction of γ-Alumina-Supported Pt Catalysts

Joo H. Kang,[†] Laurent D. Menard,[†] Ralph G. Nuzzo,*[,†] and Anatoly I. Frenkel[‡]

School of Chemical Sciences and Frederick-Seitz Materials Research Laboratory, University of Illinois, Urbana, Illinois 61801, and Department of Physics, Yeshiva University, New York, New York 10016

Received June 14, 2006; E-mail: r-nuzzo@uiuc.edu

Oxide-supported and promoted metal cluster catalysts are essential components of many of the most important chemical processes required by modern industrial economies.[1] Despite extensive research efforts seeking to elucidate the origins of the catalytic properties of such supported catalysts, fundamental understandings of their properties and mechanisms of operation remain far from complete.[1] This arises in part from the considerable structural complexity of heterogeneous catalysts, as well as the sensitivity of their kinetic activities to such features as surface area, porosity, defect sites, and quantum size and physicochemical effects of the oxide support on the electronic structure of the cluster.[2]

In this report, we demonstrate using data from X-ray absorption spectroscopy (XAS) that the support/cluster interactions in a Pt on γ-alumina catalyst results in the surprising behavior of an apparent negative thermal expansion (NTE)—the marked contraction of the Pt−Pt bonding distances with increasing temperature, over temperatures ranging from 165 to 573 K. Negative thermal expansion is uncharacteristic of close-packed metals (and the majority of materials) in their bulk form because the anharmonicity of the interatomic potential results in a greater mean interatomic distance at higher temperatures.[3]

A highly monodisperse sample of supported Pt clusters (1 wt % Pt) was prepared by impregnating the Pt^{2+} precursor, $[Pt(NH_3)_4(OH)_2 \cdot H_2O]$, on γ-Al_2O_3 without calcination and reducing it with H_2 at 573 K to remove the ligands and form metallic clusters. As evidenced in scanning transmission electron microscopy (STEM) images, this protocol generates an exceptionally narrow distribution of ~0.9 nm diameter supported Pt clusters (Figure 1). The cluster sizes were characterized on the more precise basis of the number of atoms per cluster using quantitative, atom-counting STEM measurements.[4] The supported Pt clusters were determined to be hemispherical in shape (see Supporting Information) and consist of a major population (≥90%) containing 12 ± 5 atoms and a minor population (10%) containing 35 ± 7 atoms, the overall average being 15 ± 9 atoms.

We collected high S/N Pt L_3 X-ray absorption spectra at various temperatures for both supported Pt clusters and a Pt foil standard. Data for the reduced Pt clusters were collected using two different background gases in the in situ cell:[5] the first set taken under a flowing H_2 atmosphere and the second under an ultrahigh purity He atmosphere. Hydrogen adsorbed on the Pt clusters was desorbed prior to making the latter measurements by heating the sample to 573 K in a flowing He background.

Figure 2a displays the Pt−Pt (first shell) bond lengths as a function of temperature as determined from the extended X-ray absorption fine structure (EXAFS) analysis for the Pt foil standard, Pt clusters under H_2 (Pt−H/Al_2O_3), and bare Pt clusters under He (Pt/Al_2O_3). Also included in the figure are previously reported data for 2.4 nm Pt nanoparticles on a carbon black support to illustrate the support-specific nature of the observed thermal effects.[5] The EXAFS analysis was limited to the first nearest neighbor single-scattering path and performed using the IFEFFIT package as previously described, taking account of anharmonicity of the pair-potentials by utilizing the third cumulant in the analysis.[5,6]

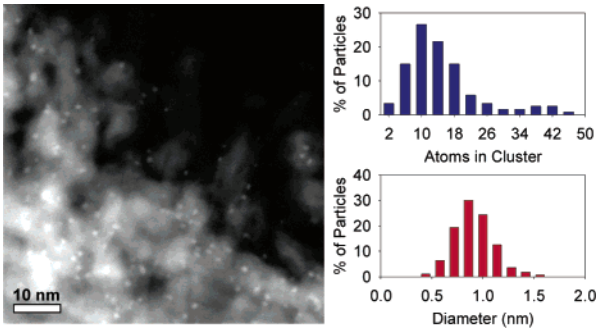

Figure 1. Representative dark-field STEM image of 1% Pt on γ-Al_2O_3. The top histogram shows the distribution of cluster atom counts (15 ± 9 atoms), and the bottom histogram displays the distribution of cluster diameters (0.9 ± 0.2 nm).

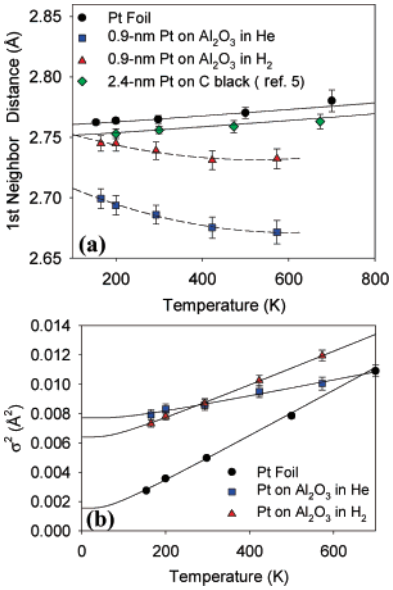

Figure 2. Temperature-dependent XAS data for a sample of 1% Pt supported on γ-Al_2O_3 and a Pt foil reference. (a) Temperature-dependent Pt−Pt first nearest neighbor distances of the Pt clusters supported on γ-Al_2O_3, previously reported 2.4 nm Pt nanoparticles on carbon black (ref 5), and a Pt foil reference. The solid lines correspond to the bulk Pt thermal expansion measured by X-ray diffraction (see text). The dotted lines are fits made using a quadratic functional form. (b) The mean-square relative displacement of the supported Pt clusters and Pt foil standard as a function of temperature. The solid lines are fits using a correlated Einstein model.

[†] University of Illinois.
[‡] Yeshiva University.

10.1021/ja064207p CCC: $33.50

Significant scattering contributions from the support (either Pt−O or Pt−Al) are not evidenced in these data. The Pt foil and Pt nanoparticles on carbon exhibit thermal expansion in Pt−Pt bonding distances in excellent agreement with X-ray diffraction measurements, with an average linear thermal expansion coefficient over the temperature range measured of 1.1×10^{-5} K^{-1} for the foil.[7]

The average first-shell coordination number determined by EXAFS for the Pt/Al_2O_3 clusters is 5.5 ± 0.2 (i.e., lower than the bulk value of 12), a result consistent with the mean 15-atom hemispherical cluster structure revealed by STEM.[5] The Pt/Al_2O_3 clusters show a significant Pt−Pt bond-length contraction from the bulk value (~3% at 293 K). Similar bond-length contractions for small metal clusters have been reported and typically attributed to the unsaturated coordination environment of the metal atoms.[5,8] What is most interesting about the present data, however, is the temperature-dependent bond-length changes they reveal for the Pt/Al_2O_3 clusters, which clearly display a substantial thermal contraction. A linear fit suggests a thermal coefficient of -2.5×10^{-5} K^{-1}, although the true functional form is clearly non-monotonic. Adsorption of hydrogen on the Pt clusters results in a Pt−Pt bond-length relaxation (as observed in previous experimental and theoretical studies), but the bond lengths are still contracted from the bulk values (by ~1% at 293 K).[9] The $Pt-H/Al_2O_3$ clusters also exhibit a thermal contraction, but the effect is less dramatic (-1.3×10^{-5} K^{-1}) than that seen for the bare nanoparticles.

The EXAFS analysis reveals additional intriguing details regarding the effect of temperature on nanoparticle structure. Figure 2b shows the mean-square relative displacements (Debye−Waller factors) of the Pt−Pt bond lengths, σ^2, plotted as a function of temperature. The solid lines in the plot are fits of the Debye−Waller factors using a correlated Einstein model.[10] The Pt foil shows a low static disorder parameter (0.00017 ± 0.00008 Å^2), as expected for a bulk metal, and an Einstein temperature of 179 ± 2 K, in close agreement with literature values (~180 K).[5,7] The Pt/Al_2O_3 clusters show the greatest static disorder (0.0069 ± 0.0003 Å^2), and this disorder is relaxed somewhat upon H_2 passivation (0.0052 ± 0.0002 Å^2). The Einstein temperatures determined for the Pt clusters are 207 ± 6 K for $Pt-H/Al_2O_3$ and 298 ± 24 K for Pt/Al_2O_3, values that are unprecedentedly high (see below).

The high-amplitude, low-frequency vibrational modes that are present in more exotic materials that display NTE (such as cubic zirconium tungstate) do not exist in fcc metals, precluding a simple vibrational origin to the thermal bond contractions noted here.[3,11] In addition, the support-specific nature of the effect indicates that it is not solely due to the nanoscale dimensions of the Pt clusters. This suggests that an explanation for the observed behavior must be due to an electronic effect, a conclusion supported by the X-ray absorption near edge structure (XANES) spectra (see Supporting Information). In the case of Pt on Al_2O_3, we believe that the observed thermal contraction is consistent with a temperature-mediated transfer of charge from the support to the Pt clusters due to their bonding at specific vacancy sites.[12] This charge transfer is greatest at lower temperatures due to the anharmonic nature of the metal−support interaction potential, creating a coulombic repulsion that partially compensates the bond contractions that result as a consequence of the finite cluster size. This suggests that the interatomic potential becomes deeper at high temperatures, and as a result, the mean-square relative displacement is expected to increase less dramatically than it would were no charge-transfer effects present. As predicted, slopes of the plots of $\sigma^2(T)$ for both $Pt-H/Al_2O_3$ and Pt/Al_2O_3 clusters are less than that of the Pt foil, with the effect being greatest for the unpassivated Pt/Al_2O_3 (Figure 2b). It would thus appear that the anomalously large Einstein temperatures reported above arise as a consequence of the convolution of the dynamical contributions and the temperature-dependent charge-transfer effects.

Current work is underway to provide a theoretical understanding of the Pt/Al_2O_3 interaction. The lack of any observable Pt−O or Pt−Al scattering suggests that bonds to the support are highly disordered and/or (less likely in our view) few in number, consistent with particle anchoring at support oxygen vacancy sites. We note that recent ab initio studies of Pt(111) films on α-alumina surfaces show charge transfer from the support when the Al_2O_3 surface is Al-terminated (slightly electropositive) and from the Pt when the Al_2O_3 surface is O-terminated (slightly electronegative).[2e]

In conclusion, the thermally mediated interaction between a γ-Al_2O_3 support and sub-nanometer Pt clusters results in an unexpected thermal contraction of the Pt−Pt bond lengths. We believe this is a general effect relevant to bonding interactions of Pt with this support, applying even in cases where larger cluster sizes would obscure signatures of support-mediated effects within more bulk-like responses. This observation has broad implications for heterogeneous catalysis since the impacts on energetics it suggests must also bear on catalytic activity, as well.

Acknowledgment. This work was sponsored in part by grants from the U.S. Department of Energy (DEFG02-03ER15476 to R.G.N. and DEFG02-03ER15477 to A.I.F.). Experiments were carried out at the Frederick Seitz Materials Research Laboratory at the University of Illinois at Urbana−Champaign and at the Advanced Photon Source at Argonne National Laboratory (UNICAT beamline 33BM), both partially supported by the U.S. DOE.

Supporting Information Available: Detailed procedures for the XAS experiments, quantitative STEM results, XANES spectra, and EXAFS spectra and fitting results. This material is available free of charge via the Internet at http://pubs.acs.org.

References

(1) (a) Rase, H. F. *Handbook of Commercial Catalysts: Heterogeneous Catalysts*; CRC Press: Boca Raton, FL, 2000. (b) Henry, C. R. *Surf. Sci. Rep.* **1998**, *31*, 231.
(2) (a) Valden, M.; Lai, X.; Goodman, D. W. *Science* **1998**, *281*, 1647. (b) Schubert, M. M.; Hackenberg, S.; van Veen, A. C.; Muhler, M.; Plzak, V.; Behm, R. J. *J. Catal.* **2001**, *197*, 113. (c) Fu, Q.; Saltsburg, H.; Flytzani-Stephanopoulos, M. *Science* **2003**, *301*, 935. (d) Eichler, A. *Phys. Rev. B* **2005**, *71*, 125418. (e) Cooper, V. R.; Kolpak, A. M.; Yourdshahyan, Y.; Rappe, A. M. *Phys. Rev. B* **2005**, *72*, 081409.
(3) Barrera, G. D.; Bruno, J. A. O.; Barron, T. H. K.; Allan, N. L. *J. Phys.: Condens. Matter* **2005**, *17*, R217.
(4) (a) Singhal, A.; Yang, J. C.; Gibson, J. M. *Ultramicroscopy* **1997**, *67*, 191. (b) Yang, J. C.; Bradley, S.; Gibson, J. M. *Mater. Charact.* **2003**, *51*, 101. (c) Menard, L. D.; Gao, S.-P.; Xu, H.; Twesten, R. D.; Harper, A. S.; Song, Y.; Wang, G.; Douglas, A. D.; Yang, J. C.; Frenkel, A. I.; Nuzzo, R. G.; Murray, R. W. *J. Phys. Chem. B* **2006**, *110*, 12874.
(5) Frenkel, A. I.; Hills, C. W.; Nuzzo, R. G. *J. Phys. Chem. B* **2001**, *105*, 12689.
(6) Newville, M. *J. Synchrotron Radiat.* **2001**, *8*, 322.
(7) *Thermophysical Properties of Matter*; Plenum Press: New York, 1975; Vol. 12.
(8) (a) Balerna, A.; Bernieri, E.; Picozzi, P.; Reale, A.; Santucci, S.; Burattini, E.; Mobilio, S. *Phys. Rev. B* **1985**, *31*, 5058. (b) Reifsnyder, S. N.; Otten, M. M.; Sayers, D. E.; Lamb, H. H. *J. Phys. Chem. B* **1997**, *101*, 4972.
(9) (a) Lytle, F. W.; Greegor, R. B.; Marques, E. C.; Sandstrom, D. R.; Via, G. H.; Sinfelt, J. H. *J. Catal.* **1985**, *95*, 546. (b) Ankudinov, A. L.; Rehr, J. J.; Low, J.; Bare, S. R. *Phys. Rev. Lett.* **2001**, *86*, 1642. (c) Hammer, B.; Nørskov, J. K. *Nature* **1995**, *376*, 238.
(10) Frenkel, A. I.; Rehr, J. J. *Phys. Rev. B* **1993**, *48*, 585.
(11) Mary, T. A.; Evans, J. S. O.; Vogt, T.; Sleight, A. W. *Science* **1996**, *272*, 90.
(12) (a) Ealet, B.; Gillet, E. *Surf. Sci.* **1996**, *367*, 221. (b) Giordano, L.; Goniakowski, J.; Pacchioni, G. *Phys. Rev. B* **2001**, *64*, 075417.

JA064207P